Anal. Chem. **2006,** *78,* 7197−7205

Protein Nanopatterns and Biosensors Using Gold Binding Polypeptide as a Fusion Partner

Tae Jung Park,[†] Sang Yup Lee,*[,†,‡] Seok Jae Lee,[†] Jong Pil Park,[†] Kwang Suk Yang,[†] Kyung-Bok Lee,[§] Sungho Ko,[∥] Jong Bae Park,[⊥] Taekeun Kim,[⊥] Seong Kyu Kim,[⊥] Yong Bum Shin,[#] Bong Hyun Chung,[#] Su-Jin Ku,[¶] Do Hyun Kim,[†] and Insung S. Choi[£]

Metabolic and Biomolecular Engineering National Research Laboratory, Department of Chemical and Biomolecular Engineering (BK21 program), BioProcess Engineering Research Center, and Center for Ultramicrochemical Process Systems, Korea Advanced Institute of Science and Technology (KAIST), Daejeon 305-701, Korea, Department of BioSystems and Bioinformatics Research Center, KAIST, Daejeon 305-701, Korea, Glycomics Team, Korea Basic Science Institute (KBSI), Daejeon 305-333, Korea, Korea Materials & Analysis Corp. (K-MAC), Daejeon 305-380, Korea, BioMEMS Team, Department of New Technology and Analysis, National Nanofab Center, Daejeon 305-806, Korea, Department of Chemistry, Sungkyunkwan University, Suwon 440-746, Korea, BioNanotechnology Research Center, Korea Research Institute of Bioscience and Biotechnology (KRIBB), Daejeon 305-333, Korea, and Department of Chemistry, KAIST, Daejeon 305-701, Korea

An efficient strategy for immobilizing proteins on a gold surface was developed by employing the gold binding polypeptide (GBP) as a fusion partner. Using the enhanced green fluorescent protein (EGFP), severe acute respiratory syndrome coronavirus (SARS-CoV) envelope protein (SCVme), and core streptavidin (cSA) of *Streptomyces avidinii* as model proteins, specific immobilization of the GBP-fusion proteins onto the gold nanoparticles and generation of protein nanopatterns on the bare gold surface were demonstrated. The GBP-fused SCVme bound to gold nanoparticles successfully interacted with its antibody and showed changes in absorbance and color, allowing efficient diagnosis of SARS-CoV. The fusion proteins could be successfully immobilized on the gold surface by nanopatterning and microcontact printing as examined by atomic force microscopy and surface plasmon resonance analysis. The poly(dimethylsiloxane) microfluidic channels were created on the gold surface and were used for antigen−antibody and DNA−DNA interaction studies. Specific immobilization of GBP−EGFP fusion protein and its interaction with the antibody in the microchannels could be demonstrated. By immobilizing the DNA probe through the use of GBP-fused cSA, specific hybridization of the target DNA prepared from *Salmonella* could also be achieved. The GBP-fusion method allows immobilization of proteins onto the gold surface without surface modification and in bioactive forms suitable for studying protein−protein, DNA−DNA, and other biomolecular interaction studies. Furthermore, these studies can be carried out in a microfluidic system, which allows high-throughput analysis of biomolecular interactions.

Patterning and immobilization of biomolecules on solid substrates have become important for various applications in diagnostics, drug discovery, and biosensors.[1−4] Microcontact printing (μCP),[5] photolithography,[6] and dip-pen nanolithography[7] are good methods for patterning proteins on glass, polymer, and metal substrates. Generally, these methods require surface modification for specific immobilization of proteins, which is complicated and often causes random orientation of proteins.[8−13] Other immobilization methods are based on the interaction between the protein amine groups and the aldehyde, epoxide, and carboxylic acids groups on the surface. A similar strategy was demonstrated by Whitesides and co-workers, who used a mixed self-assembled monolayers (SAMs) of nitrilotriacetic acid and triethylene glycol-terminated alkanethiols on gold.[14] Possible drawbacks of this approach is the necessity for the synthesis of oligo(ethylene

* To whom correspondence should be addressed. Phone: +82-42-869-3930. Fax: +82-42-869-8800. E-mail: leesy@kaist.ac.kr.

[†] Korea Advanced Institute of Science and Technology (KAIST).
[‡] Department of BioSystems and Bioinformatics Research Center, KAIST.
[§] Korea Basic Science Institute (KBSI).
[∥] National Nanofab Center.
[⊥] Sungkyunkwan University.
[#] Korea Research Institute of Bioscience and Biotechnology (KRIBB).
[¶] Korea Materials & Analysis Corp. (K-MAC).
[£] Department of Chemistry, KAIST.

(1) Jang, C.; Stevens, B. D.; Phillips, R.; Calter, M. A.; Ducker, W. A. *Nano Lett.* **2003**, *3*, 691−694.
(2) Smith, J. C.; Lee, K.; Wang, Q.; Finn, M. G.; Johnson, J. E.; Mrksich, M.; Mirkin C. A. *Nano Lett.* **2003**, *3*, 883−886.
(3) Blawas, A. S.; Reichert, W. M. *Biomaterials* **1998**, *19*, 595−609.
(4) Chen, C. S.; Mrksich, M.; Huang, S.; Whitesides, G. M.; Ingber, D. G. *Science* **1997**, *276*, 1425−1428.
(5) Lahiri, J.; Ostuni, E.; Whitesides, G. M. *Langmuir* **1999**, *15*, 2055−2060.
(6) Xia, Y.; Whitesides, G. M. *Angew. Chem.* **1998**, *110*, 568−594.
(7) Lee, K.; Park, S.; Mirkin, C. A.; Smith, J. C.; Mrksich, M. *Science* **2002**, *295*, 1702−1705.
(8) Matsui, H.; Porrata, P.; Douberly, G. E. *Nano Lett.* **2001**, *1*, 461−464.
(9) Sato, K,; Hosokawa, K.; Maeda, M. *J. Am. Chem. Soc.* **2003**, *125*, 8102−8103.
(10) Veiseh, M.; Zareie, M. H.; Zhang, M. *Langmuir* **2002**, *18*, 6671−6678.
(11) Kim, K.; Jang, M.; Yang, H.; Kim, E.; Kim, Y. T.; Kwak, J. *Langmuir* **2004**, *20*, 3821−3823.
(12) Davis, J. J.; Bruce, D.; Canters, G. W.; Crozier, J.; Hill, H. A. O. *Chem. Commun.* **2003**, 576−577.
(13) Terrettaz, S.; Ulrich, W.; Vogel, H., Hong, Q.; Dover: L. G.; Lakey, J. H. *Protein Sci.* **2002**, *11*, 1917−1925.
(14) Sigal, G. B.; Bamdad, C.; Barberis, A.; Strominger, J.; Whitesides, G. M. *Anal. Chem.* **1996**, *68*, 490−497.

10.1021/ac060976f CCC: $33.50 © 2006 American Chemical Society
Published on Web 09/09/2006

Table 1. Bacterial Strains and Plasmids Used in This Study

strain or plasmid	relevant characteristics	source
strains		
Streptomyces avidinii	ATCC 27419	ATCC[a]
Escherichia coli XL1-Blue	*recA1, endA1, gyrA96, thi, hsdR17, suppE44,relA1, l⁻, lac⁻*, F′[*proAB lacI*^{q} lacZrM15, Tn*10* (tet)^r]	Stratagene[b]
Salmonella typhimurium	KCCM 40253	KCCM[c]
plasmids		
pEGFP	Ap^r, *lac* promoter, *egfp*	Clontech[d]
pTrc99A	4.2 kb, Ap^r; *trc* promoter	Pharmacia[e]
pTrc-EGFP	4.8 kb, Ap^r; EGFP, pTrc99A derivative	this study
pTGE	5.0 kb, Ap^r; GBP-EGFP-6His, pTrc99A derivative	this study
pTGESCVme	5.4 kb, 6His-GBP-EGFP−SCVme, pTrc99A derivative	this study
pTGEcSA	5.4 kb, 6His-GBP-EGFP-cSA, pTrc99A derivative	this study

[a] American Type Culture Collection, Manassas, VA. [b] Stratagene Cloning Systems, La Jolla, CA. [c] Korea Culture Center of Microorganisms, Seoul, Korea. [d] BD Biosciences Clontech, Palo Alto, CA. [e] Amersharm Pharmacia Biotech, Uppsala, Sweden.

glycol)-terminated alkanethiols and the instability of thiol SAMs due to the slow oxidation of thiolated anchor. In the quest for the polypeptides that can bind to the inorganic surface with high affinity, Brown[15] carried out studies on the structural prediction of gold binding polypeptide (GBP). Then, the specific GBPs that are able to bind to the gold lattice were selected.[16−18] Interestingly, none of the GBPs contained cysteine residue, generally known to form a covalent bond with gold. The binding of GBP to gold is thought to be independent of thiol linkage and thus offers a new way of interaction between protein and a gold surface. These findings led us to develop protein nanopatterns and biological sensors by using GBP as a fusion partner.

In this paper, we report the development of a simple procedure for immobilizing proteins onto the gold surface by a GBP-fusion method. We first show that GBP-fusion proteins can be specifically immobilized on a gold surface. Then, the GBP-fusion proteins were immobilized onto gold nanoparticles for subsequent colorimetric assays. Using the same specific binding principle, protein nanopatterns could be generated on a gold surface. Having developed an efficient protein immobilization method using the GBP-fusion system, we next show that surface plasmon resonance (SPR) analysis can be employed for the convenient detection of biomolecular interactions on a gold surface. We finally show that this immobilization and detection system can be applied for high-throughput assays of protein−protein as well as DNA−DNA interactions in microfluidic devices.

EXPERIMENTAL SECTION

Chemicals. Unless otherwise stated, all chemical reagents were purchased from Sigma (St. Louis, MO). Rabbit anti-GFP polyclonal antibody was obtained from Molecular Probes (Eugene, OR). Poly(dimethylsiloxane) (PDMS) substrates were made using Sylgard 184 silicon elastomer kit (Dow Corning, Midland, MI).

Construction of Expression Vectors for GBP-EGFP-6His, 6His-GBP-EGFP-SCVme and 6His-GBP-EGFP-cSA Fusion Proteins. All bacterial strains and plasmids used in this study are listed in Table 1. Polymerase chain reaction (PCR) experiments were performed with a PCR Thermal Cycler MP TP 3000 (Takara Shuzo Co., Shiga, Japan) using a High Fidelity PCR System (Boehringer Mannheim, Mannheim, Germany). Restriction enzymes and DNA modifying enzymes were purchased from New England Biolabs (Berverly, MA). The DNA sequences of all clones were confirmed by automatic DNA sequencer (ABI Prism model 377, Perkin-Elmer Co.).

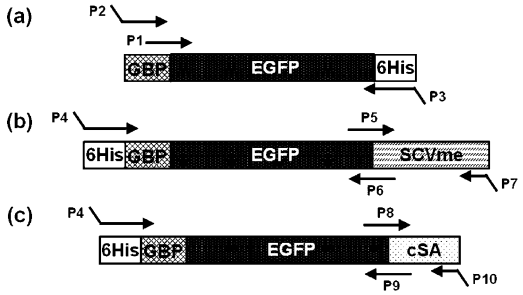

Figure 1. Synthesis of (a) GBP-EGFP-6His, (b) 6His-GBP-EGFP-SCVme, and (c) 6His-GBP-EGFP-cSA fusion genes by overlap PCR. Abbreviations: GBP, gold binding polypeptide; EGFP, enhanced green fluorescent protein; 6His, 6 histidine; SCVme, the SARS-CoV membrane-envelope chimera protein; cSA, core streptavidin. Primer sequences are shown in Table 2.

Enhanced green fluorescent protein (EGFP) from the jellyfish, *Aequorea victoria*, was used as a model protein for the convenient monitoring of protein immobilization. As shown in Figure 1a, the DNA fragments encoding GBP-fused EGFP were obtained by overlapping PCR amplification using the plasmid pEGFP (BD Biosciences Clontech, Palo Alto, CA) that contains the EGFP gene as a template. Six histidine (6His) residues were introduced for the easy purification of fusion proteins by immobilized metal affinity chromatography. For the cloning and expression of the GBP-EGFP-6His fusion gene, several PCR experiments were carried out using the primers listed in Table 2. The DNA fragment encoding incomplete GBP fused to EGFP-6His was first obtained by PCR amplification using the primers P1 and P3 and the plasmid pEGFP as a template. Then, the primers P2 and P3 were used to amplify the DNA fragment encoding the complete GBP-EGFP-6His gene using the first PCR product as a template (Figure 1a). The PCR product was digested with *Nco*I and *Hin*dIII and ligated

(15) Brown, S. *Nat. Biotechnol.* **1997**, *15*, 269−272.
(16) Sarikaya, M.; Tamerler, C.; Jen, A. K. Y.; Schulten, K.; Baneyx, F. *Nat. Mater.* **2003**, *2*, 577−585.
(17) Soh, N.; Tokuda, T.; Watananbe, T.; Mishima, K.; Imato, T.; Masadome, T.; Asano, Y.; Okutani, S.; Niwa, O.; Brown, S. *Talanta* **2003**, *60*, 733−745.
(18) Braun, R.; Sarikaya, M.; Schulten, K. *J. Biomater. Sci. Polym. Ed.* **2002**, *13*, 747−757.

Table 2. Oligonucleotides Used for PCR Amplification

no. primer	sequences[a] (5′ → 3′)
P1	GGTAAAACGCAAGCCACGTCTGGTACGATTCAATCTATGCACGGTAAAACCCAA CGACGGCGGTACCATTCAGTCTGTGAGCAAGGGCGAGGAG
P2	GCGAATTCCATGGGCAAAACCCAGGCGACCAGCGGCACC ATCCAGAGCATGCATGGTAAAACGCAAGCCACGTCT
P3[b]	CGGAATTCAAGCTTA*ATGGTGATGGTGATGGTG*CTTGTACAGCTCGTCCATG
P4[b]	GCGAATTCCATGGG*CCACCATCACCATCACCAT*GGCAAAACCCAGGCGACCA
P5	GGCATGGACGAGCTGTACAAGAATCGGAACAGGTTTTTGT
P6	ACAAAAACCTGTTCCGATTCTTGTACAGCTCGTCCATGCC
P7	CGGAATTCAAGCTTTTAGACCAGAAGATCAGGAAC
P8	CATGGACGAGCTGTACAAGGGCATCACCGGCACCTG
P9	CAGGTGCCGGTGATGCCCTTGTACAGCTCGTCCATG
P10	TAGAAGCTTGCTCAGCTTACGGCTTCACCTTGGTGA
1585Fw[c]	TTGTACACACCGCCCGTC
23BR[c]	TTCGCCTTTCCCTCACGGTACT

[a] The restriction enzyme sites are indicated by underlines. [b] The sequence for six histidine is shown in italic. [c] These are the primers for amplifying the target DNA from *S. typhimurium* as reported previously.[24]

into the same sites of pTrc99A (Pharmacia Biotech, Uppsala, Sweden) to make pTGE.

For the construction of the 6His-GBP-EGFP-SCVme fusion gene, the DNA fragments encoding EGFP and the severe acute respiratory syndrome coronavirus (SARS-CoV) membrane-envelope fusion gene (SCVme) were amplified by PCR as we previously reported.[19] The DNA fragment encoding 6His-GBP-EGFP was first amplified by PCR using the primers P4 and P6 and the plasmid pTGE as a template. The DNA fragment encoding SCVme was amplified by using the primers P5 and P7. Finally, the 6His-GBP-EGFP-SCVme fusion gene was amplified with primers P4 and P7 using the above PCR products as templates (Figure 1b). The 6His-GBP-EGFP-SCVme fusion gene obtained by PCR was digested with *Nco*I and *Hin*dIII and ligated into the same sites of pTrc99A to make pTGESCVme.

For the construction of the 6His-GBP-EGFP-cSA fusion gene, the DNA fragments encoding EGFP and core streptavidin (cSA) of *Streptomyces avidinii* were amplified by PCR as we previously reported.[20] The DNA fragment encoding 6His-GBP-EGFP was first amplified by PCR with the primers P4 and P9 using pTGE as a template. The DNA fragment encoding cSA was amplified with the primers P8 and P10 using the genomic DNA of *S. avidinii* as a template. Finally, the 6His-GBP-EGFP-cSA fusion gene was amplified with primers P4 and P10 using the above PCR products as templates (Figure 1c). The 6His-GBP-EGFP-cSA fusion gene obtained by PCR was digested with *Nco*I and *Hin*dIII and ligated into the same sites of pTrc99A to make pTGEcSA.

Production of Fusion Proteins. Recombinant *Escherichia coli* XL1-Blue strains harboring pTrc-EGFP, pTGE, pTGESCVme, and pTGEcSA were cultivated in 250-mL flasks containing 100 mL of LB medium (tryptone 10 g/L, yeast extract 5 g/L, NaCl 5 g/L) supplemented with ampicillin (50 μg/mL) in a shaking incubator at 37 °C and 200 rpm. Cell growth was monitored by measuring the absorbance at 600 nm (OD_{600}; DU Series 600 spectrophotometer, Beckman, Fullerton, CA). At an OD_{600} of 0.6, isopropyl β-D-thiogalactopyranoside (Sigma) was added to a final concentration of 1 mM for the induction of gene expression from the *trc* promoter. Then, cells were further cultivated for 4 h and were harvested by centrifugation at 10000*g* for 10 min at 4 °C. Cells were disrupted by sonication (Braun Ultrasonics Co, Danbury, CT) for 1 min at 40% output. After centrifugation at 16000*g* for 10 min at 4 °C, the supernatant containing soluble proteins was obtained and used for further experiments. Since the GBP-EGFP-6His, 6His-GBP-EGFP-SCVme, and 6His-GBP-EGFP-cSA fusion proteins contain a six-histidine tag, they could be simply purified using Ni-chelating resin (Qiagen, Valencia, CA) without further purification steps. Protein concentration was determined by Bradford's method using bovine serum albumin (BSA; Sigma) as a standard.

UV/Visible Spectroscopy. Optical properties of the GBP-EGFP-6His fusion proteins bound to the monodisperse gold nanoparticles (nominal diameter of 20 nm, Sigma) were characterized by UV/visible absorption spectrum analysis (Cary 100 spectrophotometer, Varian Inc., Palo Alto, CA). For the binding of GBP-EGFP-6His fusion proteins to gold nanoparticles, the purified fusion proteins (20 μL of 0.1 mg/mL solution) were added to gold nanoparticle solution (80 μL of 0.01% $HAuCl_4$ solution) and incubated at 25 °C for 30 min. Unbound fusion proteins were removed by washing with phosphate-buffered saline (PBS) solution 3 times. Rabbit anti-GFP polyclonal antibodies (20 μL of 100 μg/mL solution, Molecular Probes) were added to the gold nanoparticles-GBP-EGFP-6His protein complexes. UV/visible absorption spectrum analysis was performed within the 400−700-nm wavelength range. For the binding of 6His-GBP-EGFP-SCVme fusion proteins to gold nanoparticles, the purified fusion proteins (20 μL of 0.1 mg/mL solution) were added to gold nanoparticle solution (80 μL of 0.01% $HAuCl_4$ solution) and incubated at 25 °C for 30 min. For the colorimetric assay of SCVme, 0.06% $HAuCl_4$ solution was used instead. Unbound fusion proteins were removed by washing with PBS solution 3 times. For antigen−antibody interaction studies, rabbit anti-SCVme polyclonal antibodies[19] (20 μL of 100 μg/mL solution, Peptron, Daejeon, Korea) were added to the gold nanoparticles-6His-GBP-EGFP-SCVme protein complexes. As a negative control, BSA (20 μL of 0.1 mg/mL solution) was added instead of antibodies.

SPR Spectroscopy. The binding of GBP-fusion protein on a gold surface was characterized by SPR using a BIAcore3000

(19) Lee, S. J.; Park, J. P.; Park, T. J.; Lee, S. Y.; Lee, S.; Park, J. K. *Anal. Chem.* **2005**, *77*, 5755−5759.
(20) Park, J. P.; Lee, S. J.; Park, T. J.; Lee, K. B.; Choi, I. S.; Lee, S. Y.; Kim, M. G.; Chung, B. H. *Biotechnol. Bioprocess Eng.* **2004**, *9*, 137−142.

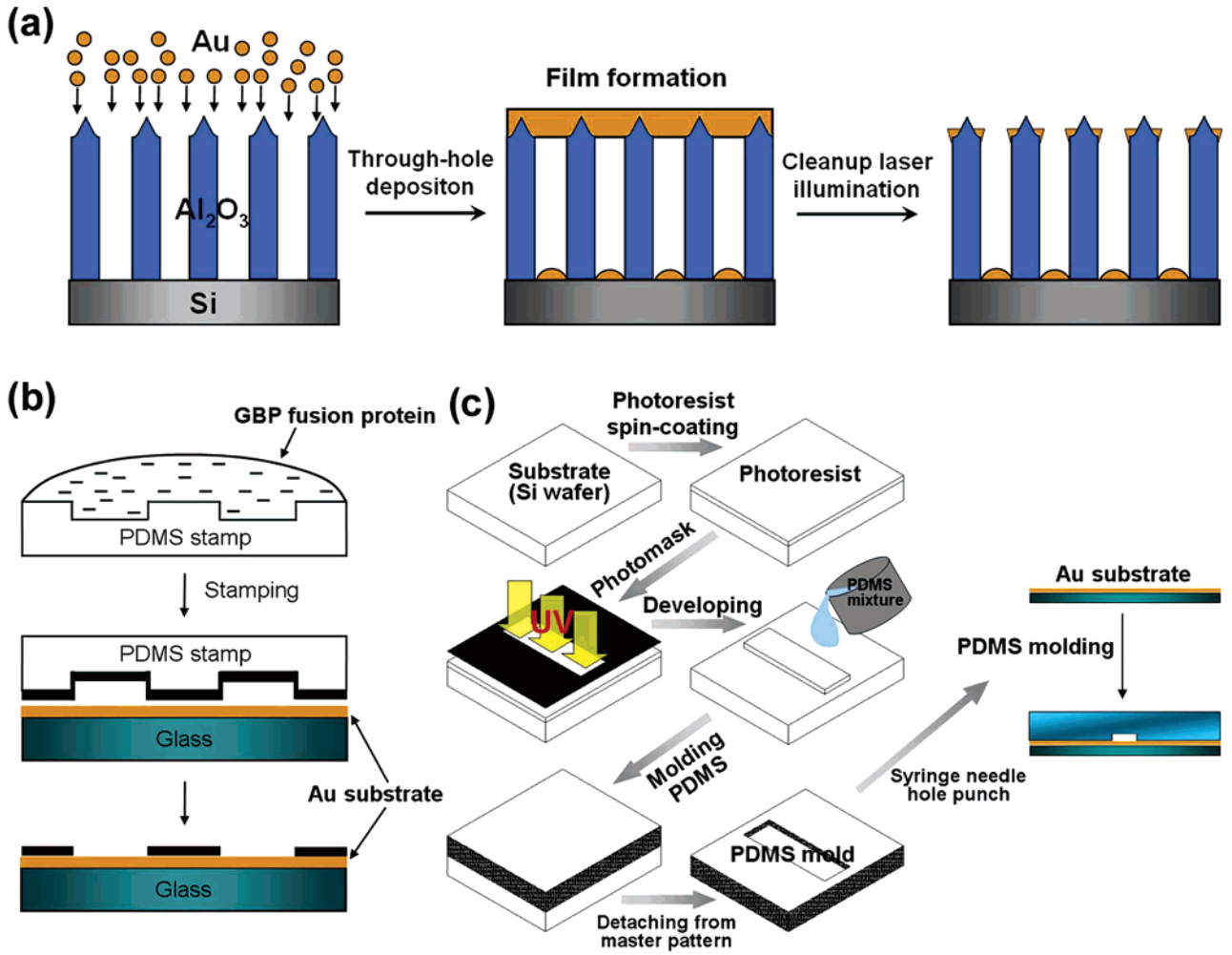

Figure 2. Schematic diagrams of (a) laser-ablated deposition method for the generation of gold nanopatterns, (b) microcontact printing procedure using the PDMS stamp, and (c) the fabrication process of the PDMS microfluidic device by photolithography.

(Biacore, Uppsala, Sweden). The gold sensor chip was attached to a separate chip carrier for easy assembly after surface coating and was inserted into the BIAcore SPR system. All experiments were conducted in PBS solution at a flow rate of 5 μL/min at 25 °C, and all sensorgrams were fitted globally using BIA evaluation software. Fifty microliters of GBP-EGFP-6His fusion protein (0.1 mg/mL) or EGFP protein (negative control; 0.1 mg/mL) was loaded onto the chip using a liquid-handling micropipet. After protein binding, the surface of gold chip was washed and equilibrated with PBS solution.

SPR Imaging Analysis. All SPR imaging experiments were performed with an SPR imager apparatus (SPR*i*, K-MAC, Daejeon, Korea). An incoherent light source (a 150-W quartz tungsten−halogen lamp, Schott) was used for excitation as previously reported.[21] Briefly, p-polarized collimated white light incident on a prism/Au/thin film/buffer flow cell assembly was set at a fixed angle. Reflected light from this assembly was passed through a band-pass filter centered at 830 nm and collected by a CCD camera (Sony). The Scion Image Beta 4.0.2 software (Scion Corp., Frederick, MD) was used to analyze the images.

Fabrication of Gold Nanostructures. Gold nanodot arrays were fabricated by modifying the silicon substrate using the laser-ablated deposition method as previously reported.[22] The schematic diagram of the laser-assisted deposition process is shown in Figure 2a. Gold nanospheres were deposited through a porous anodized aluminum oxide (AAO) mask using a pulsed laser deposition process in a vacuum. Gold nanoparticles were ablated by pulsed Q-switched Nd:YAG lasers (Surelite-II, Photonic Solutions, Edinburgh, UK). The laser beam was focused onto the target to fabricate a regular exposed area. Then, the laser pulse was illuminated onto the surface of the gold-deposited AAO mask by the cleanup laser fluence. The gold nanopattern was fabricated onto the curved-shaped AAO cells and the Si bottom surface. Then, the AAO surface was covered with gold having a 30-nm thickness. The gold nanospheres had average diameter of 50 nm. The prenanopatterned gold substrate was incubated with 0.1 mg/mL GBP-EGFP-6His solution containing 0.1% (w/v) BSA, 0.02% (v/v) Tween 20, 50 mM sodium phosphate, and 300 mM NaCl (pH 8.0) for 30 min. Then, the substrate was rinsed 3 times with deionized water.

Microcontact Printing (μCP) of GBP-EGFP-6His Fusion Protein. PDMS stamps were prepared using a Sylgard 184 silicone elastomer as previously reported.[23] The schematic diagram of the microcontact printing procedure is shown in Figure

(21) Jung, J. M.; Shin, Y.-B.; Kim, M.-G.; Ro, H.-S.; Jung, H.-T.; Chung, B. H. *Anal. Biochem.* **2004**, *330*, 251−256.

(22) Kim, C. H.; Park, J. B.; Jee, H. G.; Lee, S. B.; Boo, J.-H.; Kim, S. K.; Yoo, J.-B.; Lee, J. S.; Lee, H. S. *J. Nanosci. Nanotechnol.* **2005**, *5*, 306−312.

2b. After curing for 6 h at 60 °C, the PDMS stamp was peeled off the master. The PDMS stamp was designed to have micrometer-sized relief features (circles of 50 μm in diameter). For μCP of fusion proteins, PDMS stamps were sonicated in 50% (v/v) absolute ethanol for 10 min, rinsed with deionized water 3 times, and dried under the stream of argon. After inking with 0.1 mg/mL GBP-EGFP-6His solution containing 0.1% (w/v) BSA, 0.02% (v/v) Tween 20, 50 mM sodium phosphate, and 300 mM NaCl (pH 8.0), the PDMS stamp was brought into contact with the gold substrate. A small amount of force was applied to make a better contact between the stamp and gold substrate. The stamp was carefully removed after 10 min, and the protein-immobilized gold substrate was washed with PBS solution and deionized water.

Fabrication of Microfluidic Device. The microfluidic channels were fabricated on PDMS polymer as previously reported.[4] The schematic diagram for fabricating microfluidic device is shown in Figure 2c. Briefly, the desired master pattern was made on a silicon wafer with a negative photoresist (SU-8 50, Microlithography Chemical Corp., Newton, MA), which was spin-coated at 500 rpm for 30 s and exposed to UV light. Replicas were formed from a 1:10 mixture of PDMS curing agent and prepolymer (Sylgard 184, Dow Corning, Miland, MI), which were degassed under vacuum and poured onto the master pattern. The PDMS mixture was then cured for 2 h at 70 °C before it was removed from the silicon wafer. Finally, the PDMS mold having the microchannels (a width of 100 μm and a depth of 50 μm) were peeled off from the template. Both ends of the mold were pierced with a syringe needle for introducing protein solutions into the channels. Sample reservoirs (1 mm in diameter) were created by cutting out the circular ends of the channels with a hole punch. The PDMS mold was manually brought onto the gold-coated glass substrate.

AFM Imaging. All AFM analysis were carried out with the NanoScope IV MultiMode system (Digital Instruments, Santa Barbara, CA) in tapping mode using Nanoprobe TESP cantilever tips (Digital Instruments) with a spring constant of 50 N/m and resonance frequencies of 240 kHz. Images were acquired in an ambient atmosphere (40−50% relative humidity) at a speed of 3−4 kHz and a resolution of 512 × 512 pixels.

DNA Preparation for the Detection of *Salmonella*. To prepare hybridization samples, PCR was performed with the 1585Fw and 23BR primer pair using the genomic DNA from *Salmonella typhimurium* KCCM 40253 as a template.[24] PCR was performed in 50 μL of solution containing 1× PCR buffer, 0.2 mM dNTPs, 1 unit of r*Taq* polymerase (Takara Shuzo Co., Shiga, Japan), and 10 pmol each of forward and reverse primers under the following conditions: 30 cycles of 94 °C for 4 min; 10 cycles of 94 °C for 50 s, 56 °C for 50 s, and 72 °C for 1 min 10 s; 20 cycles of 94 °C for 50 s, 58 °C for 50 s, 72 °C for 1 min 10 s, and a final extension at 72 °C for 5 min. The PCR product (1144 bp) was confirmed by 2% (w/v) agarose gel electrophoresis. The 3′-terminus of *Salmonella*-specific probe DNA (5′-GCC TGA ATC AGC ATG TGT GTT AGT GGA AGC GTC TGG AAA G-3′) was modified with biotin for the interaction with 6His-GBP-EGFP-cSA fusion protein.

Protein−Protein and DNA−DNA Interaction Studies in Microfluidic Channels. For studying protein−protein interactions on gold surface in the PDMS microfluidic channels, the GBP-EGFP-6His fusion protein (0.1 mg/mL) was introduced. After washing with PBS to remove unbound proteins, the anti-GFP antibody (0.1 mg/mL) was subsequently added. Then, the channels were washed with PBS to remove unbound antibodies and dried in the air. The microfluidic channels were analyzed by SPR imaging as described above. All samples and buffers were flown through the microfluidic channels by using the syringe pump (NE-1600, New Era Pump Systems Inc.). BSA (1%, w/v) was used as a negative control.

To study DNA−DNA interactions on a gold surface within the PDMS microfluidic channels, the 6His-GBP-EGFP-cSA fusion protein (0.1 mg/mL) was introduced. The channels were washed with PBS to remove unbound fusion proteins. The biotinylated probe DNA (100 nM), which can detect pathogenic *Salmonella*, was subsequently introduced. For the specific binding of biotinylated DNA probes to cSA, the reaction mixtures were incubated at 30 or 37 °C for 1 h. After the reaction, the channels were washed with PBS to remove unbound probe DNA molecules. Then, the denaturated target DNA (100 nM) from *S. typhimurium* was introduced into the microfluidic channels and incubated at 30 or 37 °C for 1 h. After washing with PBS to remove unbound target DNA and drying in the air, the microfluidic channels were analyzed by SPR imaging as described above. The 6His-GBP-EGFP-cSA fusion protein and DNA molecules were flown through the channels by using the syringe pump. Again, BSA (1%, w/v) was used as a negative control.

RESULTS AND DISCUSSION

Immobilization of GBP-Fusion Proteins on Gold Nanoparticles and Bioassays. The purified GBP-EGFP-6His fusion proteins were added into gold nanoparticle solution and incubated at 25 °C for 30 min. The UV/visible absorption spectra before and after the addition of fusion proteins to colloidal gold nanoparticles are shown in Figure 3a. The surface plasmon band shifted from 520 nm to a longer wavelength of 524 nm, and the absorbance decreased as GBP-EGFP-6His was bound to the gold nanoparticles. Subsequent binding of the anti-GFP antibodies further shifted the surface plasmon band to 525 nm and decreased the absorbance. These observations indicate the aggregation of the gold nanoparticles caused by the binding of GBP-EGFP-6His fusion proteins and subsequent binding of antibodies. Formation of gold nanoparticle aggregates became evident to the naked eyes as the solution color changed. As shown in Figure 3b, the bare gold nanoparticle solution appeared as a pink color, while those bound with GBP-EGFP-6His fusion proteins and GBP-EGFP-6His plus anti-GFP antibodies showed a pink-to-yellow and yellow-to-purple colorimetric transition in 1 min.

To examine the possibility of employing this system in colormetric diagnosis of SARS, the SCVme antigen was immobilized onto the gold nanoparticles. The UV/visible absorption spectra before and after the addition of 6His-GBP-EGFP-SCVme fusion proteins to colloidal gold nanoparticles are shown in Figure 3c. As in the previous case, the surface plasmon band appeared

(23) Lee, K.-B.; Kim, D. J.; Lee, Z.-W.; Woo, S. I.; Choi, I. S. *Langmuir* **2004**, *20*, 2531−2535.

(24) Keum, K. C.; Yoo, S. M.; Lee, S. Y.; Chang, K. H.; Yoo, N. C.; Yoo, W. M.; Kim, J. M.; Choi, J. Y.; Kim, J. S.; Lee, G. *Mol. Cell. Probes* **2006**, *20*, 42−50.

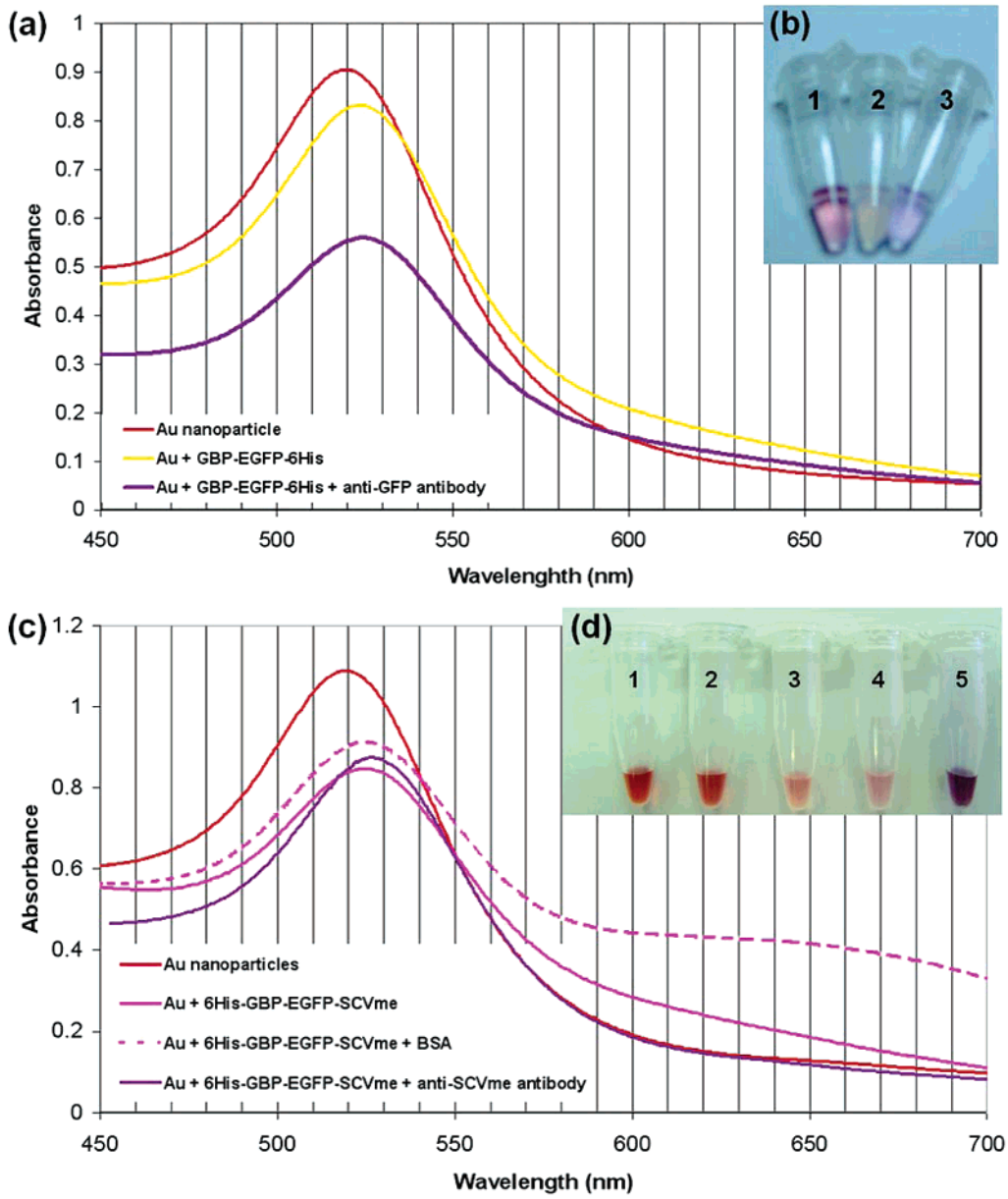

Figure 3. Immobilization of GBP-fusion proteins on colloidal gold nanoparticles and colorimetric assay of protein−protein interactions. (a) UV/visible absorption spectra of bare gold nanoparticles as a negative control (red line; 520-nm peak), gold nanoparticles plus GBP-EGFP-6His fusion proteins (yellow line; 524-nm peak), gold nanoparticles plus GBP-EGFP-6His fusion proteins and anti-GFP antibodies (purple line; 525-nm peak). (b) Colorimetric detection of GBP-EGFP-6His fusion protein binding to the gold nanoparticles and subsequent antibody binding: 1, bare gold nanoparticles as a negative control; 2, gold nanoparticles plus GBP-EGFP-6His fusion proteins; 3, gold nanoparticles plus GBP-EGFP-6His fusion proteins and anti-GFP antibodies. (c) UV/visible absorption spectra of bare gold nanoparticles as a negative control (red line; 519-nm peak), gold nanoparticles plus 6His-GBP-EGFP-SCVme fusion proteins (pink line; 525-nm peak), gold nanoparticles plus 6His-GBP-EGFP-SCVme fusion proteins and BSA (dotted pink line; 525-nm peak), and gold nanoparticles plus 6His-GBP-EGFP-SCVme fusion proteins and anti-SCVme antibodies (purple line; 527-nm peak). (d) Colorimetric detection of 6His-GBP-EGFP-SCVme fusion protein binding to gold nanoparticles and subsequent antibody binding: 1, bare gold nanoparticles; 2, bare gold nanoparticles plus BSA; 3, gold nanoparticles plus 6His-GBP-EGFP-SCVme fusion proteins; 4, gold nanoparticles plus 6His-GBP-EGFP-SCVme fusion proteins and BSA; 5, gold nanoparticles plus 6His-GBP-EGFP-SCVme fusion proteins and anti-SCVme antibodies.

at longer wavelength with lower absorbance by the binding of fusion proteins to the gold nanoparticles. The surface plasmon band shifted to a longer wavelength as the anti-SCVme antibodies were bound to the 6His-GBP-EGFP-SCVme fusion proteins on the gold nanoparticles. For increasing the colorimetric intensities, the gold nanoparticles at a high concentration (80 μL of 0.06% $HAuCl_4$ solution) were used. As shown in Figure 3d, the binding of anti-SCVme antibodies to the 6His-GBP-EGFP-SCVme changed the color to purple, which could be clearly observed with naked eyes. On the other hand, the color transition was not observed when BSA instead of anti-SCVme antibody was added (sample 4 in Figure 3d). These results suggest that the colorimetric immunoassay of SARS-CoV is possible by using the 6His-GBP-EGFP-SCVme fusion proteins immobilized on the gold nanoparticles. Furthermore, the aggregation of gold nanoparticles upon GBP-fusion protein binding was relatively rapid (1 min). Therefore, this

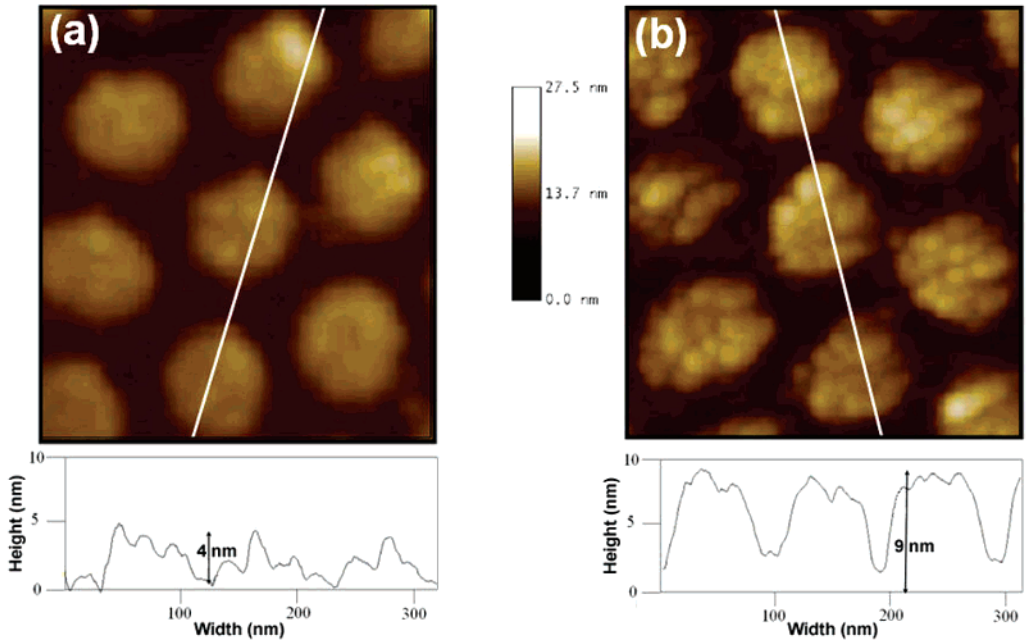

Figure 4. AFM images of GBP-EGFP-6His fusion proteins deposited onto the gold nanodots arrays: (a) nanoarrays of gold nanodots and (b) nanopatterns of GBP-EGFP-6His fusion proteins deposited onto the gold nanodot arrays. The cross-sectional contours below the images are the average height differences of the individual scan lines contained in the area.

system employing the GBP-fusion proteins and gold nanoparticles should be valuable for rapid, reliable, and colorimetric assays of antigen−antibody and other protein−protein interactions.

Generation of Protein Nanopatterns. Since GBP-fusion proteins can specifically bind to the gold surface, we examined the possibility of generating protein nanopatterns through the binding of GBP-fusion proteins onto the prenanopatterned gold surface. After immobilization of GBP-EGFP-6His fusion proteins on the nanopatterned bare gold surface, the surface morphologies were examined by AFM. The successful generation of GBP-EGFP-6His fusion protein nanopatterns was observed, indicating the specific binding of GBP-fusion proteins to the nanopatterned gold regions only. Figure 4 shows the representative high-resolution images of gold nanopatterns and nanopatterned proteins in a scan area of 300 × 300 nm. The size of each gold nanopattern was about 50−60 nm in diameter. It could be seen that the GBP-EGFP-6His fusion proteins formed a dense monolayer on the corresponding gold nanopatterns. Ormo et al. reported that GFP has a 4.2 nm long cylindrical structure with a molecular weight (MW) of ~27 000.[25] The GBP-EGFP-6His has a MW of ~32 000. Thus, the length of GBP-EGFP-6His fusion protein has a dimension of ~5 nm. The line profile of the GBP-EGFP-6His fusion proteins bound to the gold nanopatterns showed repeated 4−5-nm height differences from the substrate surface, indicating that the GBP-EGFP-6His fusion proteins were immobilized as a highly ordered monolayer showing uniform thickness. In our previous paper, we reported fabrication of versatile nanostructures that are made of gold nanodots and nanospheres or rings on several substrates.[21] By combining these nanostructures and GBP-fusion proteins, various protein nanoarrays and nanostructures can be developed.

SPR Analysis of GBP-Fusion Protein Binding to the Gold Surface. After proving that GBP-fusion proteins could be functionally immobilized and nanopatterned on a gold surface, A more convenient and efficient method for detecting biomolecular interactions was needed. Most protein assays developed so far rely on various detection methods requiring enzymatic reactions or fluorescent tags.[21,26] In contrast, SPR is a label-free and surface-sensitive spectroscopic technique used to study bioaffinity interactions on gold thin films by measuring changes in the local index of refraction upon adsorption.[21] To examine whether protein−protein interaction studies can be carried out by combining the GBP-fusion approach with SPR, the GBP-EGFP-6His fusion proteins were flown over the gold sensor chip to monitor their binding affinity. The dynamic and specific binding of fusion proteins onto the gold sensor chip could be directly monitored in real time by SPR spectroscopy (Figure 5). A sharp increase in

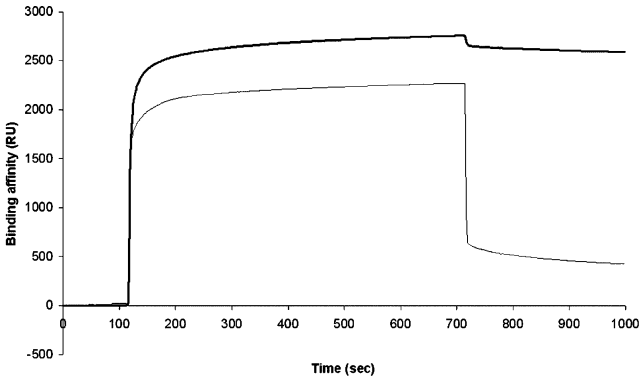

Figure 5. SPR sensorgrams showing the specific immobilization of GBP-EGFP-6His fusion proteins onto the gold sensor chip. The GBP-EGFP-6His fusion protein (boldface line) and EGFP (light line) were introduced at the flow rate of 5 μL/min. After protein binding, the surface of gold chip was washed with PBS solution.

(25) Ormo, M.; Cubitt, A. B.; Kallio, K.; Gross, L. A.; Tsien, R. Y.; Remington, S. J. *Science* **1996**, *273*, 1392−1395.

(26) Wegner, G. J.; Wark, A. W.; Lee, H. J.; Codner, E.; Saeki, T.; Fang, S.; Corn, R. M. *Anal. Chem.* **2004**, *76*, 5677−5684.

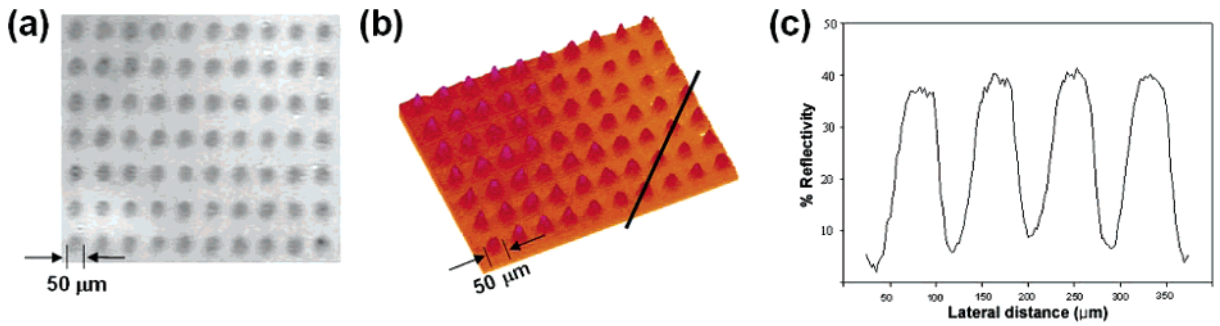

Figure 6. SPR imaging analysis of GBP-fusion proteins immobilized onto gold surface by microcontact printing: (a) two-dimensional and (b) three-dimensional images of GBP-EGFP-6His fusion protein nanopatterns having the feature of 50-μm circles. (c) Line profiles of the immobilized GBP-fusion proteins scanned through the line in (b).

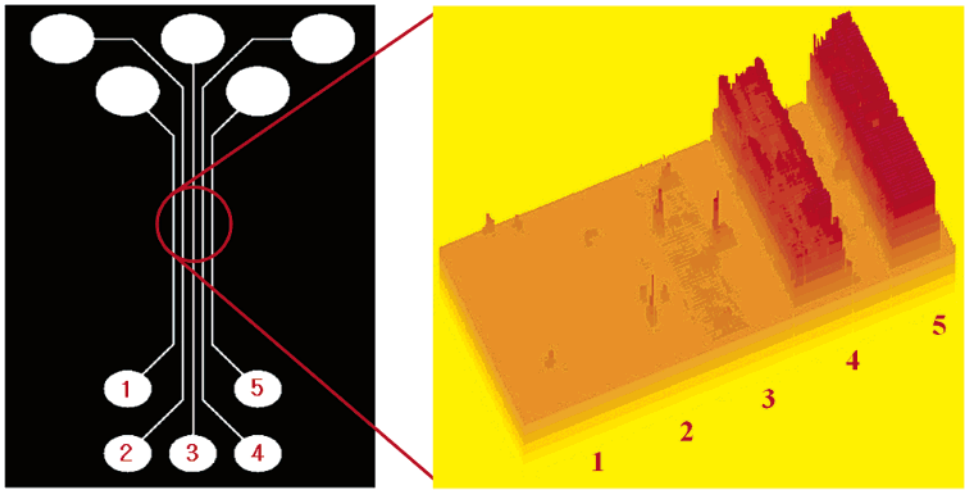

Figure 7. Protein−protein interaction studies in microchannels examined by SPR imaging. Dimensions of the microfluidic channels: 100-μm width, 50-μm depth, and 50-μm spacing between the channels. Samples flown through the channels: channel 1, bare gold surface; channel 2, binding buffer; channel 3, 1% (w/v) BSA in PBS buffer followed by anti-GFP antibody (0.1 mg/mL); channel 4, GBP-EGFP-6His fusion proteins (0.1 mg/mL); channel 5, GBP-EGFP-6His fusion proteins (0.1 mg/mL) followed by anti-GFP antibody (0.1 mg/mL).

the SPR signal was observed upon introducing the GBP-EGFP-6His protein solution onto the sensor chip. About 94% of the injected total GBP-EGFP-6His fusion proteins were bound onto the gold surface. Most of GBP-EGFP-6His remained bound to the gold surface after washing with PBS buffer. A little decline in SPR signal during washing is due to the removal of unbound GBP-EGFP-6His proteins from the gold surface. However, when EGFP instead of GBP-EGFP-6His was flown over the gold sensor chip, the SPR signal sharply decreased after washing with the PBS buffer. About 15% of EGFP protein was nonspecifically bound to the gold surface, which is common for most proteins. Strong binding of GBP-fusion protein onto the gold sensor chip suggests that various protein−protein and antigen−antibody interaction studies can be performed using this system.

To examine whether the GBP-fusion protein system can be used in real-time, SPR-based, protein−protein interaction studies, we carried out the following experiments. The GBP-EGFP-6His fusion proteins were immobilized on the bare gold surface by μCP with a PDMS stamp that has relief features of 50-μm circles. After micropatterning of the GBP-EGFP-6His fusion proteins on the gold surface, the substrate was incubated in a solution of 0.1% (w/v) BSA, 0.02% (v/v) Tween 20, 50 mM sodium phosphate, and 300 mM NaCl (pH 8.0) for 30 min. Then, the gold substrate was rinsed 3 times with distilled water. Successful micropatterning of GBP-fusion proteins was verified by the two-dimensional (Figure 6a) and three-dimensional (Figure 6b) SPR imaging, indicating the specific immobilization of GBP-EGFP-6His fusion proteins onto the gold surface. However, when the gold substrate was printed with the native EGFP as an ink, no micropatterns could be observed (data not shown). A line profile taken from this SPR differential reflectance image showed that the GBP-EGFP-6His fusion proteins were uniformly and specifically immobilized only on the micropatterned regions, whereas their nonspecific adsorption to the other regions was not observed (Figure 6c).

High-Throughput Detection of Biomolecular Interactions in Microfluidic Channels. High-throughput assays are required in many applications involving drug, target, and library screening. After finding that SPR assay could be successfully used for biomolecular interaction studies on a gold surface, we next examined whether the GBP-fusion protein system can be used for high-throughput detection of biomolecular interactions. We fabricated the PDMS microfluidic channels by the procedure shown in Figure 2c. By using this microfluidic system with microchannels having a width of 100 μm and a depth of 50 μm, SPR imaging was performed to study protein−protein interactions on the gold chip. As shown in Figure 7, the specific binding of the GBP-EGFP-6His fusion proteins could be observed in channel 4. Subsequent binding of the anti-GFP antibodies to the GBP-

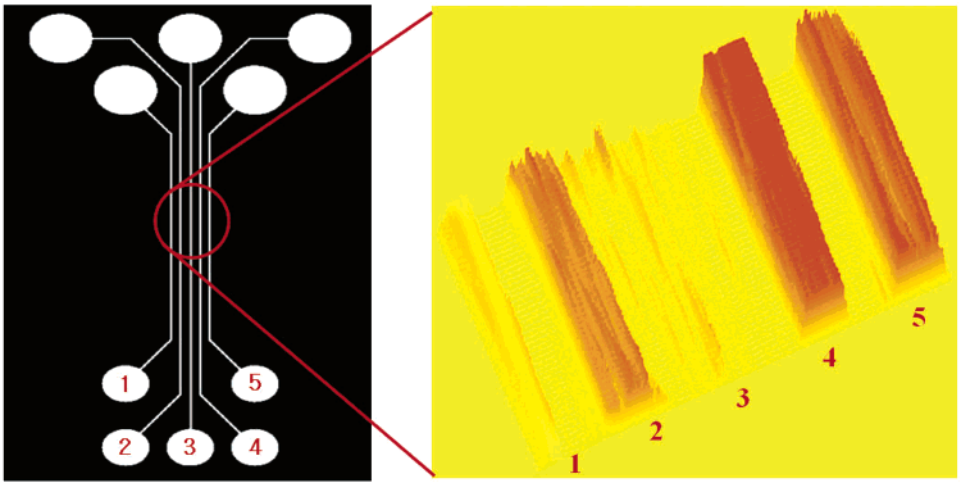

Figure 8. DNA−DNA interaction studies in microchannels examined by SPR imaging. Dimensions of the microfluidic channels: 100-μm width, 50-μm depth, and 50-μm spacing between the channels. Samples flown through the channels: channel 1, bare gold surface; channel 2, 6His-GBP-EGFP-cSA fusion proteins (0.1 mg/mL); channel 3, the mixtures of 1% (w/v) BSA and biotinylated probe DNA; channel 4, 6His-GBP-EGFP-cSA (0.1 mg/mL) and biotinylated probe DNA followed by the target DNA (hybridization at 30 °C); channel 5, 6His-GBP-EGFP-cSA (0.1 mg/mL) and biotinylated probe DNA followed by the target DNA (hybridization at 37 °C).

EGFP-6His fusion proteins increased the signal as shown in channel 5. However, when the anti-GFP antibodies were added into channel 3, which have BSA introduced, no signal was observed. These results indicate that the GBP-fusion protein binding to the gold microchannels is highly specific. Furthermore, the fusion proteins remained functional in the microchannels as demonstrated by successful antigen−antibody interactions.

To further investigate whether this system can be used to detect DNA−DNA interactions within the microfluidic channels on gold chip, the 6His-GBP-EGFP-cSA fusion proteins were applied into the microfluidic channels. The biotinylated probe DNA, which can detect pathogenic *S. typhimuriun*, was subsequently introduced. When the denaturated target DNA from *S. typhimuriun*. was introduced into the microfluidic channels 4 and 5 and incubated at different temperatures, the DNA−DNA interactions could successfully be detected (Figure 8). The signal intensities in channels 4 and 5 were much stronger than that in channel 2, indicating the successful hybridization of DNA. Hybridization was more efficient at 30 °C as indicated by the stronger signal in channel 4 (Figure 8). No visible SPR image was obtained with BSA and biotinylated probe DNA in channel 3. These results suggest that DNA−DNA interaction studies can be carried out in gold microchannels by the combined use of GBP-cSA fusion protein and biotinylated DNA probes. This method does not require any surface modification and allows simultaneously monitoring of multiple DNA−DNA interactions in microfluidic channels and thus allows high-throughput detection of target DNAs.

CONCLUSIONS

A simple GBP-fusion protein method was developed for the controlled immobilization of proteins with high selectivity and specificity on a bare gold surface in micro-to-nanoscale resolutions. The GBP-fusion proteins attached to gold surface remained active, which is critical for the development of high-performance biosensors. Using the GBP-fusion proteins and gold nanoparticles, the colorimetric assay of protein−protein interaction was possible. As demonstrated by successful antigen−antibody and DNA−DNA interaction studies, this method not only provides convenient yet specific immobilization of biomolecules onto the gold surface but also allows simple yet accurate bioassays by SPR. The specific binding of GBP-fusion proteins on the nanopatterned gold surface and the generation of direct GBP-fusion protein micropatterns suggest that various nanobiosensor devices can be manufactured. Furthermore, these assays could be carried out in microfluidic channels, which will allow high-throughput bioassays of multiple samples. Production of various GBP-fusion proteins for desired applications is possible by simply cultivating recombinant microorganisms, which is another advantage of this system. This platform technology should be useful for various nanobiotechnological applications in the fields of biosensors and diagnostics.

ACKNOWLEDGMENT

This work was supported by the R&D program for Regional Development from the Ministry of Commerce, Industry and Energy (S.Y.L.), by the KOSEF through the Center for Ultramicrochemical Process Systems (S.Y.L.), and by the Center for Nanotubes and Nanostructured Composites (S.K.K.).

Received for review May 27, 2006. Accepted August 11, 2006.

AC060976F